Available online at www.sciencedirect.com
ScienceDirect
Journal of Sound and Vibration 305 (2007) 457–466
JOURNAL OF SOUND AND VIBRATION
www.elsevier.com/locate/jsvi

Free vibration analysis of circular and annular sectorial thin plates using curve strip Fourier *p*-element

Li Yongqiang*, Li Jian

College of Science, Northeastern University, Shenyang 110004, China

Received 12 July 2006; received in revised form 30 March 2007; accepted 8 April 2007
Available online 29 June 2007

Abstract

A curve strip Fourier *p*-element for free vibration analysis of circular and annular sectorial thin plates is presented. The element transverse displacement is described by a fixed number of polynomial shape functions plus a variable number of trigonometric shape functions. The polynomial shape functions are used to describe the element's nodal displacements and the trigonometric shape functions are used to provide additional freedom to the edges and the interior of the element. With the additional Fourier degrees of freedom (dof) and reduce dimensions, the accuracy of the computed natural frequencies is greatly increased. Results are obtained for a number of circular and annular sectorial thin plates and comparisons are made with exact, the curve strip Fourier *p*-element, the proposed Fourier *p*-element and the finite strip element. The results clearly show that the curve strip Fourier *p*-element produces a much higher accuracy than the proposed Fourier *p*-element, the finite strip element.

1. Introduction

The problem of the flexural vibration of circular and annular sectorial thin plates is of some practical importance, since components with sectorial geometries are widely used in curved bridge decks and aeronautical structures, etc.

For uniform, isotropic, sectorial plates with both radial edges simply supported, exact free vibration solutions are obtainable for arbitrary boundaries conditions at the circumferential edge, as mentioned by Leissa [1]. These solutions utilize the Bessel functions of the first kind, $J_\mu(kr)$ and $I_\mu(kr)$, where μ is typically not an integer. An equivalent procedure was later used by Rubin [2], however, solutions to the equation of motion were developed by the Frobenius method, instead of using Bessel functions. For sectorial plates with free circumferential edge, exact solutions have been given by Westmann [3]. Kim and Dickinson [4] also presented results for annular and circular, thin, sectorial plates subject to certain complicating effects. In addition to these studies presenting exact solutions, the Rayleigh–Ritz method has also been used to determine approximate natural frequencies for some case [3–5].

*Corresponding author. Tel.: +86 2483681645.
E-mail address: lyq525@sohu.com (L. Yongqiang).

0022-460X/$ - see front matter © 2007 Elsevier Ltd. All rights reserved.
doi:10.1016/j.jsv.2007.04.022

The finite element method has been used by Khurasia and Rawtani [6] and Cheung [7] to study the vibration of circular plates. The accuracy of the solution may be improved in two ways for the finite element method. The first is the *h*-version to refine the finite element mesh and the second is the *p*-version to increase the order of polynomial shape functions for a fixed mesh. Zienkiewicz and Taylor [8] concluded that, in general, *p*-version convergence is more rapid per degree of freedom introduced. The Fourier *p*-elements are popular for the dynamic problems. Leung and Chan [9] gave the trigonometric shape functions for the axial vibration analysis of a two-node bar. Houmat [10] adopt sector Fourier *p*-element for the free vibration analysis of sectorial plates. The classical finite strip method, pioneered by Cheung [11] is an efficient analysis tool for structures with regular geometry and simple boundary conditions. It is a hybrid Ritz approach which combines the versatility of the finite element method and rapid convergence of the Ritz method by selecting suitable trial functions a priori. Cheung proposed the finite strip method for structural analysis of prismatic domain problems and in contrast to discretizing all domains as commonly carried out in FEM, only the transverse cross-section is discretized. Along the longitudinal coordinate, however, the functions and their differential are still continuous and smooth. Thus, the method is regarded as a semi-analytical method. The method may reduced from three dimensions to two dimensions and two dimensions to one dimension, so it can save more time and makes the calculation results are more accurate. Cheung and Chan [12] adopt finite strip method for the free vibration analysis of thin and thick sectorial plates. Mizusawa and Kajita [13] adopt spline strip method for the vibration of annular sector plates.

In the present paper, combines the finite strip method with the proposed Fourier *p*-element method, to calculate the flexural frequencies of circular and annular sectorial thin plates. The boundary conditions are considered to be any combination of classical boundary conditions.

2. Analysis

The uniform annular sectorial thin plate is imagined to be separated into a small number of curve strip Fourier *p*-element, each curve strip Fourier *p*-element having a constant thickness of its own. The coordinate system used to define the geometry of the curve strip Fourier *p*-element is shown in Fig. 1.

Considering a curve strip Fourier *p*-element defined by the sides *i* and *j*, the maximum strain energy $V_{\max}$ and the kinetic energy $T_{\max}$ have the forms

$$V_{\max} = \frac{D_0}{2}\int_{R_i}^{R_o}\int_0^{\alpha}\left[\left(\frac{\partial^2 w}{\partial r^2}\right)^2 + \left(2\mu\frac{\partial^2 w}{\partial r^2} + \frac{1}{r}\frac{\partial w}{\partial r} + \frac{1}{r^2}\frac{\partial^2 w}{\partial \theta^2}\right) \times \left(\frac{1}{r}\frac{\partial w}{\partial r} + \frac{1}{r^2}\frac{\partial^2 w}{\partial \theta^2}\right) + 2(1-\mu)\left\{\frac{\partial}{\partial r}\left(\frac{1}{r}\frac{\partial w}{\partial \theta}\right)\right\}^2\right] r\,\mathrm{d}\theta\,\mathrm{d}r, \tag{1}$$

$$T_{\max} = \frac{\rho h}{2}\int_{R_i}^{R_o}\int_0^{\alpha}\left(\frac{\partial w}{\partial t}\right)^2 r\,\mathrm{d}\theta\,\mathrm{d}r, \tag{2}$$

where D_0 denote the flexural rigidities $D_0 = Eh^3/12(1-\mu^2)$, h the thickness of curve strip Fourier *p*-element, E and μ are Young's module and Poisson ratios, where ρ is the material density.

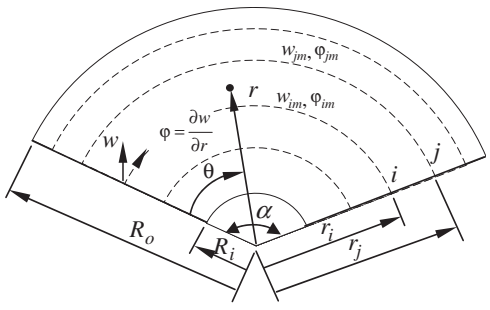

Fig. 1. An annular sectorial thin plate and curve strip Fourier *p*-element.

For free vibration, the transverse displacement w can be written as

$$w = \sum_{m=1}^{\infty} \left[N_m^e\right] \left\{\delta_m^e\right\} \sin \omega t, \tag{3}$$

where $[N_m^e]$ is the shape functions matrix of the element, and $\delta_m^e = \{ w_{im} \quad \varphi_{im} \quad w_{jm} \quad \varphi_{jm} \quad w_p \}^{\mathrm{T}}$, $p = 1, 2, \ldots$ is the vector of nodal displacement for curve strip Fourier p-element. m is numbers of nodal radius. w_{im}, φ_{im}, w_{jm}, φ_{jm} are the primary displacements by the sides i and j. w_p represent internal displacement and are to be eliminated before assembling element matrix. Leung et al. [9] adopted the Fourier enriched shape functions $f_i(\zeta) = [1 - \xi, \xi, \sin(p\pi\xi)]$, $(p = 1, 2, \ldots)$ to analyze the axial vibration of a two-node bar. The sine functions represent internal dof. When considering the flexural vibration of an annular sectorial thin plate, the appropriate shape functions matrix of the curve strip Fourier p-element method are

$$\begin{aligned}\left[N_m^e\right] &= \Theta_m(\theta)\left[1 - 3\left(\frac{r - r_i}{r_j - r_i}\right)^2 + 2\left(\frac{r - r_i}{r_j - r_i}\right)^3, (r - r_i)\left(1 - 2\frac{r - r_i}{r_j - r_i} + \left(\frac{r - r_i}{r_j - r_i}\right)^2\right),\right.\\ &\quad \left.\times \left(\frac{r - r_i}{r_j - r_i}\right)^2 \left(3 - 2\frac{r - r_i}{r_j - r_i}\right), \frac{(r - r_i)^2}{r_j - r_i}\left(\frac{r - r_i}{r_j - r_i} - 1\right), \frac{r - r_i}{r_j - r_i}\left(1 - \frac{r - r_i}{r_j - r_i}\right) \sin\left(\frac{r - r_i}{r_j - r_i} p\pi\right)\right]\\ &= \left[N_1, N_2, N_3, N_4, N_{4+p}\right], \quad (p = 1, 2, \ldots),\end{aligned} \tag{4}$$

where $\Theta_m(\theta)$ is a series to satisfy the boundary conditions, in which

$$\begin{aligned}N_1 &= \Theta_m(\theta)\left\{1 - 3\left(\frac{r - r_i}{r_j - r_i}\right)^2 + 2\left(\frac{r - r_i}{r_j - r_i}\right)^3\right\}, \quad N_2 = \Theta_m(\theta)(r - r_i)\left(1 - 2\frac{r - r_i}{r_j - r_i} + \left(\frac{r - r_i}{r_j - r_i}\right)^2\right),\\ N_3 &= \Theta_m(\theta)\left(\frac{r - r_i}{r_j - r_i}\right)^2 \left(3 - 2\frac{r - r_i}{r_j - r_i}\right), \quad N_4 = \Theta_m(\theta)\frac{(r - r_i)^2}{r_j - r_i}\left(\frac{r - r_i}{r_j - r_i} - 1\right),\\ N_{p+4} &= \Theta_m(\theta)\frac{r - r_i}{r_j - r_i}\left(1 - \frac{r - r_i}{r_j - r_i}\right) \sin\left(\frac{r - r_i}{r_j - r_i} p\pi\right).\end{aligned} \tag{5}$$

Due to the flexural vibration of annular sectorial plate is a truly two-dimensional problem; the shape functions $[N_m^e]$ may reduce from two dimensions to one dimension by the finite strip method [11]. For two radial edges simply supported or clamped, $\Theta_m(\theta)$ is given by

(a) two radial edges simply supported

$$\Theta_m(\theta) = \sin \frac{m\pi\theta}{\alpha}, \quad m = 1, 2, \ldots, \infty, \tag{6a}$$

(b) two radial edges clamped supported

$$\begin{aligned}\Theta_m(\theta) &= \sin \frac{\mu_m\theta}{\alpha} - \sinh \frac{\mu_m\theta}{\alpha} - \frac{\sin \mu_m - \sinh \mu_m}{\cos \mu_m - \cosh \mu_m}\left(\cos \frac{\mu_m\theta}{\alpha} - \cosh \frac{\mu_m\theta}{\alpha}\right),\\ \mu_m &= \frac{2m + 1}{2}\pi, \quad m = 1, 2, \ldots, \infty.\end{aligned} \tag{6b}$$

For the other boundary conditions, $\Theta_m(\theta)$ are given in Ref. [11].

Assumable that the motion is harmonic and inserting the expression for w into expressions for the strain energy and kinetic energy then the stiffness matrix and the mass matrix of the element are obtained by applying the principle of minimum potential energy and the Hamilton's principle, respectively

$$\left[\mathbf{K}_m^e\right] = D_0 \int_0^{\alpha} \int_{r_i}^{r_j} \left[\mathbf{B}_m^e\right]^{\mathrm{T}} [\mathbf{D}] \left[\mathbf{B}_m^e\right] r \, \mathrm{d}r \, \mathrm{d}\theta, \tag{7}$$

$$\left[\mathbf{M}_m^e\right] = \rho h \int_0^{\alpha} \int_{r_i}^{r_j} \left[N_m^e\right]^{\mathrm{T}} \left[N_m^e\right] r \, \mathrm{d}r \, \mathrm{d}\theta, \tag{8}$$

where $[\mathbf{B}_m^e]$ and $[\mathbf{D}]$ are, respectively, given in close form by

$$[\mathbf{D}] = \begin{bmatrix} 1 & \mu & 0 \\ \mu & 1 & 0 \\ 0 & 0 & (1-\mu)/2 \end{bmatrix}, \tag{9}$$

$$[\mathbf{B}_m^e] = \begin{bmatrix} N_{1,rr} & N_{2,rr} & N_{3,rr} & N_{4,rr} & N_{4+p,rr} \\ \dfrac{N_{1,\theta\theta}}{r^2} + \dfrac{N_{1,r}}{r} & \dfrac{N_{2,\theta\theta}}{r^2} + \dfrac{N_{2,r}}{r} & \dfrac{N_{3,\theta\theta}}{r^2} + \dfrac{N_{3,r}}{r} & \dfrac{N_{4,\theta\theta}}{r^2} + \dfrac{N_{4,r}}{r} & \dfrac{N_{4+p,\theta\theta}}{r^2} + \dfrac{N_{4+p,r}}{r} \\ \dfrac{2N_{1,r\theta}}{r} - \dfrac{2N_{1,\theta}}{r^2} & \dfrac{2N_{2,r\theta}}{r} - \dfrac{2N_{2,\theta}}{r^2} & \dfrac{2N_{3,r\theta}}{r} - \dfrac{2N_{3,\theta}}{r^2} & \dfrac{2N_{4,r\theta}}{r} - \dfrac{2N_{4,\theta}}{r^2} & \dfrac{2N_{4+p,r\theta}}{r} - \dfrac{2N_{4+p,\theta}}{r^2} \end{bmatrix},$$

$(p = 1, 2, \ldots).$ (10)

The expressions $N_{1,r}$, $N_{1,\theta}$, etc. are given in Appendix A.

For different boundary conditions, the concrete expression of the series $\Theta_m(\theta)$ is substituted into Eq. (10), the stiffness matrix and the mass matrix of the element is calculated.

Before assembling the elements, the internal dof can be condensed by exact dynamic condensation [14]. The stiffness matrix and the mass matrix of the element are expressed

$$[K_m^e] = \begin{bmatrix} K_{cc}^e & K_{cs}^e \\ K_{sc}^e & K_{ss}^e \end{bmatrix}_m, \tag{11}$$

$$[M_m^e] = \begin{bmatrix} M_{cc}^e & M_{cs}^e \\ M_{sc}^e & M_{ss}^e \end{bmatrix}_m, \tag{12}$$

where p and s denote the central dof and subordinate dof. The central dof denote the primary displacements w_{im}, φ_{im}, w_{jm}, φ_{jm} by the sides i and j. The subordinate dof denote the internal displacements w_p, $p = 1, 2, \ldots$. K_{cc}^e and M_{cc}^e denote the stiffness matrix and the mass matrix of the central dof for the element. K_{ss}^e and M_{ss}^e denote the stiffness matrix and the mass matrix of the subordinate dof for the element.

The dynamic matrix is expressed

$$[D_m^e] = \begin{bmatrix} D_{cc}^e & D_{cs}^e \\ D_{sc}^e & D_{ss}^e \end{bmatrix}_m = \begin{bmatrix} K_{cc}^e & K_{cs}^e \\ K_{sc}^e & K_{ss}^e \end{bmatrix}_m - \omega^2 \begin{bmatrix} M_{cc}^e & M_{cs}^e \\ M_{sc}^e & M_{ss}^e \end{bmatrix}_m, \tag{13}$$

where ω is the flexural frequency of the plate.

Condensing all internal degrees of freedom of $[K_m^e] - \omega^2[M_m^e]$ according to Leung [14] gives the condensing dynamic stiffness matrix, the dynamic stiffness matrix and the mass matrix

$$\left[\hat{D}_m^e\right] = [D_{cc}^e] - [D_{cs}^e]\left([D_{ss}^e]\right)^{-1}[D_{sc}^e], \tag{14}$$

$$\left[\hat{K}_m^e\right] = [\hat{D}_m^e] + \omega^2\left[\hat{M}_m^e\right], \tag{15}$$

$$\begin{aligned}\left[\hat{M}_m^e\right] = {} & [M_{cc}^e] - [D_{cs}^e]\left([D_{ss}^e]\right)^{-1}[M_{sc}^e] - [M_{cs}^e]\left([D_{ss}^e]\right)^{-1} \\ & \times [D_{sc}^e] + [D_{cs}^e]\left([D_{ss}^e]\right)^{-1}[M_{ss}^e]\left([D_{ss}^e]\right)^{-1}[D_{sc}^e].\end{aligned} \tag{16}$$

Based on the routine method, the global dynamic stiffness matrix and mass matrix are assembled with the condensing dynamic stiffness matrix and the mass matrix of element. Then, for free vibrations one has

$$\left([\hat{D}] - \omega^2\left[\hat{\mathbf{M}}\right]\right)\mathbf{u} = 0, \tag{17}$$

where $[\hat{D}]$ is the global dynamic stiffness matrix of the structure, $[\hat{\mathbf{M}}]$ is the global dynamic mass matrix of the structure, $\mathbf{u}$ is the eigenvector in terms of the central dof of the structure.

Table 1
Non-dimensional frequencies $\omega R_o^2\sqrt{\rho h/D_0}$ for annular sectorial thin plates with simply supported radial edges and various edge conditions on circumferential edge ($R_i/R_o = 0.2$, $\alpha = \pi/3$, $\mu = 0.3$)

Circumferential edge conditions	Source of results	dof	Mode number					
			1	2	3	4	5	6
F–F	Present	4	12.4020 (1)	47.3798 (2)	52.4684 (1)	102.1157 (3)	109.3283 (1)	122.5602 (2)
	Fourier-p 20×20	8	12.4028	47.3880	52.4643	102.1608	109.3201	122.5315
	Finite strip 20×1	4	12.4024	47.3839	52.4684	102.1444	109.3201	122.5438
	Exact [4]	–	12.40	47.38	52.47	102.1	109.3	122.6
F–S	Present	4	39.6564 (1)	92.6767 (1)	97.9866 (2)	162.9202 (1)	177.6036 (3)	183.8936 (2)
	Fourier-p 20×20	8	39.6494	92.6562	97.9497	162.9202	177.4929	183.7952
	Finite strip 20×1	4	39.6518	92.6644	97.9661	162.9202	177.5298	183.8280
	Exact [4]	–	39.66	92.68	97.99	163.0	177.6	184.0
F–C	Present	4	50.5053 (1)	108.4098 (1)	114.2036 (2)	183.2593 (1)	198.7510 (3)	205.9823 (2)
	Fourier-p 20×20	8	50.4961	108.3852	114.1585	183.2334	198.6098	205.8511
	Finite strip 20×1	4	50.5002	108.3934	114.1749	183.2334	198.6549	205.8962
	Exact [4]	–	50.51	108.4	114.2	183.3	198.8	206.0
S–F	Present	4	12.4701 (1)	47.3798 (2)	53.7026 (1)	102.1157 (3)	116.3558 (1)	122.5684 (2)
	Fourier-p 20×20	8	12.4717	47.3880	53.7026	102.1608	116.3276	122.5438
	Finite strip 20×1	4	12.4713	47.3839	53.7026	102.1444	116.3276	122.5520
	Exact [4]	–	12.47	47.38	53.70	102.1	116.4	122.6
S–S	Present	4	40.3083 (1)	97.5151 (1)	97.9907 (2)	177.6036 (3)	179.8588 (1)	183.9715 (2)
	Fourier-p 20×20	8	40.3050	97.4987	97.9538	177.4929	179.8055	183.8690
	Finite strip 20×1	4	40.3059	97.5069	97.9661	177.5298	179.8219	183.9059
	Exact [4]	–	40.31	97.52	98.00	177.6	179.9	184.0
S–C	Present	4	51.6975 (1)	114.2118 (2)	115.3886 (1)	198.7510 (3)	204.8055 (1)	206.1176 (2)
	Fourier-p 20×20	8	51.6934	114.1626	115.3640	198.6098	204.7194	205.9864
	Finite strip 20×1	4	51.6934	114.1790	115.3722	198.6549	204.7481	206.0315
	Exact [4]	–	51.70	114.2	115.4	198.8	204.8	206.1
C–F	Present	4	12.6148 (1)	47.3798 (2)	55.4084 (1)	102.1157 (3)	122.5930 (2)	122.6176 (1)
	Fourier-p 20×20	8	12.6152	47.3880	55.4043	102.1608	122.5643	122.5930
	Finite strip 20×1	4	12.6152	47.3880	55.4043	102.1444	122.5725	122.6012
	Exact [4]	–	12.61	47.38	55.41	102.1	122.6	122.6
C–S	Present	4	41.3277 (1)	97.9989 (2)	102.3740 (1)	177.6036 (3)	184.1150 (2)	191.1512 (1)
	Fourier-p 20×20	8	41.3195	97.9620	102.3453	177.4929	184.0125	191.0856
	Finite strip 20×1	4	41.3236	97.9743	102.3535	177.5298	184.0453	191.1102
	Exact [4]	–	41.33	98.00	102.4	177.6	184.1	191.2
C–C	Present	4	53.3869 (1)	114.2282 (2)	121.6827 (1)	198.7610 (3)	206.3595 (2)	217.9841 (1)
	Fourier-p 20×20	8	53.3746	114.1790	121.6376	198.6098	206.2242	217.8898
	Finite strip 20×1	4	53.3787	114.1954	121.6540	198.6549	206.2693	217.9226
	Exact [4]	–	53.39	114.2	121.7	198.8	206.4	218.0

3. Numerical examples

3.1. Free vibration of annular sectorial thin plates with simply supported radial edges

To study the accuracy of the present elements, annular sectorial thin plates with simply supported radial edges and various edge conditions on circumferential edges is studied.

The non-dimensional free vibration frequencies $\omega R_o^2\sqrt{\rho h/D}$ for annular sectorial thin plates with $\alpha = \pi/3$ using five sine terms are presented in Table 1. The nine boundary conditions are, respectively, F–F, F–S, F–C, S–F, S–S, S–C, C–F, C–S and C–C. The symbolism F–F indicates that the edges $r = R_i$ and R_o are free and free, respectively. The symbolism F–S indicates that the edges $r = R_i$ and R_o are free and simply supported, respectively. The symbolism F–C indicates that the edges $r = R_i$ and R_o are free and clamped, respectively.

The results computed by 20 curve strip Fourier p-elements with $p = 5$ are compared with the computed results of Fourier p-element method with $p = 5$ and finite strip method with a mesh of 20×1 and the exacts in Ref. [4] and are given in Table 1. The non-dimensional frequencies discrepancy between different methods and exact value are shown in Fig. 2.

It can be found that the present method can obtain very high accurate frequencies of the annular sectorial thin plates. The numbers in parentheses show the value of m in Table 1.

Table 2 gives the convergence study of the first six natural frequency parameters of an annular sectorial thin plate with simply supported on four edges by means of a different number of sine terms with 20 curve strip Fourier p-elements and compares them to the exact solution. It is shown that the computed results of the present method with $p = 5$ produces extremely good results.

3.2. Free vibration of completely free sectorial thin plates

Completely free sectorial thin plates of $R_i = 0$ having a wide range of salient and re-entrant angles ($15^\circ \leqslant \alpha \leqslant 359^\circ$) is studied. The first six modes using five sine terms were computed and are tabulated in Table 3. The results computed by 20 curve strip Fourier p-elements with $p = 5$ are compared with the exacts in Ref. [15] in Table 3. It can be found that the present method can obtain very high accurate frequencies of the sectorial thin plate.

3.3. Free vibration of circular thin plates

This example is the vibration analysis of circular thin plates with outer radius simply supported. The structure parameters of circular thin plates are inner radius $R_i = 0.0$, $\alpha = 2\pi$ and $\Theta_m(\theta) = \cos m\theta$. The

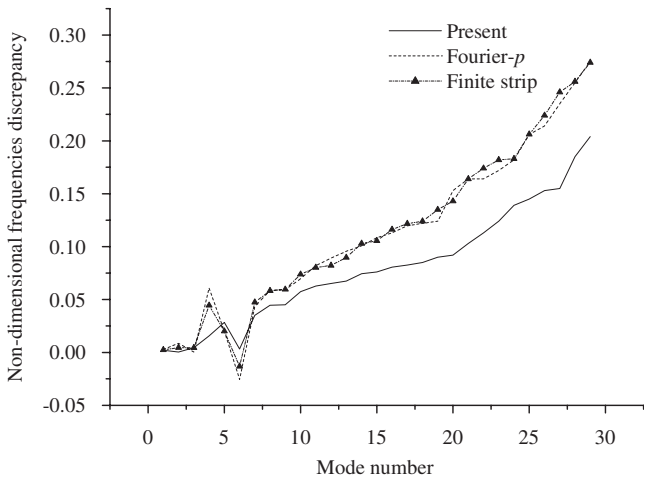

Fig. 2. The non-dimensional frequencies discrepancy between different methods and exact value.

Table 2
Comparison of the non-dimensional frequencies $\omega R_o^2\sqrt{\rho h/D_0}$ for an annular sectorial thin plate with simply supported on four edges

Mode case	1	2	3	4	5	6
Present						
$p=1$	40.3071	97.5110	97.9784	177.5667	179.8383	183.9387
$p=2$	40.3079	97.5110	97.9866	177.5831	179.8465	183.9510
$p=3$	40.3079	97.5110	97.9866	177.5913	179.8506	183.9592
$p=4$	40.3083	97.5151	97.9907	177.5995	179.8547	183.9674
$p=5$	40.3083	97.5151	97.9907	177.6036	179.8588	183.9715
$p=6$	40.3083	97.5151	97.9907	177.6036	179.8588	183.9715
Exact [4]	40.31	97.52	98.00	177.6	179.9	184.0

Table 3
Comparison of non-dimensional frequencies $\omega R_o^2\sqrt{\rho h/D_0}$ for completely free sectorial thin plates with different α ($\mu=0.3$)

α (degrees)	Source of results	Mode number					
		1	2	3	4	5	6
15	Present	27.6369	70.3993	121.9984	132.4790	213.7976	232.6224
	Leissa [15]	27.64	70.40	122.0	132.5	213.8	232.6
30	Present	27.9777	62.3093	70.9939	112.8382	128.1449	137.0017
	Leissa [15]	27.98	62.31	70.99	112.8	128.1	137.0
45	Present	28.2885	42.5783	54.2931	73.9010	95.1615	133.3360
	Leissa [15]	28.29	42.58	54.29	73.9	95.16	133.3
60	Present	27.7034	32.8702	34.3721	74.0416	74.7580	85.2058
	Leissa [15]	27.70	32.87	34.37	74.04	74.76	85.21
75	Present	21.6373	27.0986	30.5130	52.2729	72.7037	73.2901
	Leissa [15]	21.64	27.10	30.51	52.27	72.70	73.29
90	Present	16.1575	23.1765	30.5904	38.4157	57.6376	67.3194
	Leissa [15]	16.16	23.18	30.59	38.42	57.64	67.32
120	Present	10.4465	17.4783	25.0574	31.2097	37.1912	47.3570
	Leissa [15]	10.45	17.48	25.06	31.21	37.20	47.36
150	Present	7.9937	12.8309	20.1935	25.1829	31.4105	37.7464
	Leissa [15]	7.994	12.83	20.19	25.18	31.41	37.75
180	Present	6.9321	9.4969	18.0572	18.1901	29.1828	29.2045
	Leissa [15]	6.932	9.497	18.06	18.19	29.18	29.20
270	Present	4.6056	5.9946	9.2783	12.8883	17.2796	18.7018
	Leissa [15]	4.606	5.995	9.278	12.89	17.28	18.70
330	Present	3.1982	4.9148	7.9050	9.0002	13.1815	16.4270
	Leissa [15]	3.198	4.915	7.905	9.000	13.18	16.43
359	Present	2.7708	4.3019	7.6729	7.7256	11.3589	14.9113
	Leissa [15]	2.771	4.302	7.673	7.726	11.36	14.91

frequencies of circular thin plates with different Poisson ratios using 20 curve strip Fourier p-elements are computed and compared with exact solutions [16] in Table 4. m is numbers of nodal radius in Table 4. The computed results show that the curve strip Fourier-p element can obtain the very accurate results with a simple mesh and a few trigonometric terms.

Table 4
Comparison of the non-dimensional frequencies $\omega R_o^2\sqrt{\rho h/D_0}$ for circular thin plates with outer radius simply supported ($p = 5$)

μ	m	Numbers of nodal circle	Present	Exact [16]
0.1	1	1	13.63838	13.6384
		2	48.25218	48.2522
		3	102.55568	102.556
	2	1	25.37069	25.3707
		2	69.89493	69.8949
		3	134.08272	134.083
	3	1	39.72360	39.7236
		2	94.32979	94.3298
		3	168.46051	168.461
0.2	1	1	13.77051	13.7705
		2	48.36645	48.3665
		3	102.66477	102.665
	2	1	25.49346	25.4935
		2	70.00665	70.0067
		3	134.19121	134.191
	3	1	39.84157	39.8416
		2	94.44003	94.4400
		3	168.56840	168.568
0.3	1	1	13.89824	13.8982
		2	48.47886	48.4789
		3	102.77327	102.773
	2	1	25.61328	25.6133
		2	70.11698	70.1170
		3	134.29801	134.298
	3	1	39.95728	39.9573
		2	94.54898	94.5490
		3	169.67467	168.675

4. Conclusions

A curve strip Fourier p-element method for the vibration analysis of circular and annular sectorial thin plates is presented. For flexural vibration problems, the present curve strip Fourier p-element is a better choice to obtain solutions with high accuracy.

For the flexural vibrations of annular sectorial thin plates with simply supported radial edges and various edge conditions on circumferential edges, comparison with the results computed by the curve strip Fourier p-elements, the proposed Fourier p-elements, the finite strip method and the exact solutions, respectively, was carried out to examine the effectiveness. The results showed that the curve strip Fourier-p element was more accurate in predicting the natural modes than the proposed Fourier p-elements and the finite strip method. The six lowest modes of an annular sectorial thin plate with simply supported on four edges were analyzed with different number of Fourier terms. The computed results using five Fourier terms were in good agreement with the exact solutions.

For the natural frequencies of completely free sectorial thin plates having a wide range of salient and re-entrant angles, comparison with the results computed by the curve strip Fourier p-elements and the exact solutions was carried out. The computed results indicate that the curve strip Fourier p-elements can obtain very high accurate frequencies of the sectorial thin plate.

In this way, circular thin plates with outer radius simply supported were analyzed by the curve strip Fourier p-elements and the results were compared with exact solutions. The computed results show that the curve strip Fourier p-element can obtain the very accurate results with a simple mesh and a few trigonometric terms.

Acknowledgments

The author is very grateful to A.Y.T. Leung of the City University of Hong Kong for supporting this work.

Appendix A. The expressions $N_{1,r}$, $N_{1,\theta}$, etc.

$$N_{1,r}=\frac{6(r-r_i)(r-r_j)}{(r_j-r_i)^3}\Theta_m(\theta),\quad N_{2,r}=\left[1-4\frac{r-r_i}{r_j-r_i}+3\left(\frac{r-r_i}{r_j-r_i}\right)^2\right]\Theta_m(\theta),$$
$$N_{3,r}=\frac{-6(r-r_i)(r-r_j)}{(r_j-r_i)^3}\Theta_m(\theta),\quad N_{4,r}=\frac{(r-r_i)(3r-2r_j-r_i)}{(r_j-r_i)^2}\Theta_m(\theta),$$

$$N_{p+4,r}=\left[\frac{r_i+r_j-2r}{(r_j-r_i)^2}\sin\left(\frac{r-r_i}{r_j-r_i}p\pi\right)-p\pi\frac{(r-r_i)(r-r_j)}{(r_j-r_i)^3}\cos\left(\frac{r-r_i}{r_j-r_i}p\pi\right)\right]\Theta_m(\theta),$$

$$N_{1,rr}=\frac{6(2r-r_i-r_j)}{(r_j-r_i)^3}\Theta_m(\theta),\quad N_{2,rr}=\frac{2}{r_j-r_i}\left(3\frac{r-r_i}{r_j-r_i}-2\right)\Theta_m(\theta),$$
$$N_{3,rr}=\frac{-6(2r-r_i-r_j)}{(r_j-r_i)^3}\Theta_m(\theta),\quad N_{4,rr}=\frac{6r-4r_i-2r_j}{(r_j-r_i)^2}\Theta_m(\theta),$$

$$N_{p+4,rr}=\left\{\left[(p\pi)^2\frac{(r-r_i)(r-r_j)}{(r_j-r_i)^4}-\frac{2}{(r_j-r_i)^2}\right]\sin\left(\frac{r-r_i}{r_j-r_i}p\pi\right)+\frac{2p\pi(r_i+r_j-2r)}{(r_j-r_i)^3}\cos\left(\frac{r-r_i}{r_j-r_i}p\pi\right)\right\}\Theta_m(\theta),$$

$$N_{1,r\theta}=\frac{6(r-r_i)(r-r_j)}{(r_j-r_i)^3}\Theta'_m(\theta),\quad N_{2,r\theta}=\left[1-4\frac{r-r_i}{r_j-r_i}+3\left(\frac{r-r_i}{r_j-r_i}\right)^2\right]\Theta'_m(\theta),$$
$$N_{3,r\theta}=\frac{-6(r-r_i)(r-r_j)}{(r_j-r_i)^3}\Theta'_m(\theta),\quad N_{4,r\theta}=\frac{(r-r_i)(3r-2r_j-r_i)}{(r_j-r_i)^2}\Theta'_m(\theta),$$

$$N_{p+4,r\theta}=\left[\frac{r_i+r_j-2r}{(r_j-r_i)^2}\sin\left(\frac{r-r_i}{r_j-r_i}p\pi\right)-p\pi\frac{(r-r_i)(r-r_j)}{(r_j-r_i)^3}\cos\left(\frac{r-r_i}{r_j-r_i}p\pi\right)\right]\Theta'_m(\theta),$$

$$N_{1,\theta}=\Theta'_m(\theta)\left[1-3\left(\frac{r-r_i}{r_j-r_i}\right)^2+2\left(\frac{r-r_i}{r_j-r_i}\right)^3\right],$$
$$N_{2,\theta}=\Theta'_m(\theta)(r-r_i)\left[1-2\frac{r-r_i}{r_j-r_i}+\left(\frac{r-r_i}{r_j-r_i}\right)^2\right],$$
$$N_{3,\theta}=\Theta'_m(\theta)\left(\frac{r-r_i}{r_j-r_i}\right)^2\left(3-2\frac{r-r_i}{r_j-r_i}\right),\quad N_{4,\theta}=\Theta'_m(\theta)\frac{(r-r_i)^2}{r_j-r_i}\left(\frac{r-r_i}{r_j-r_i}-1\right),$$

$$N_{p+4,\theta}=\Theta'_m(\theta)\frac{r-r_i}{r_j-r_i}\left(1-\frac{r-r_i}{r_j-r_i}\right)\sin\left(\frac{r-r_i}{r_j-r_i}p\pi\right),$$

$$N_{1,\theta\theta} = \Theta''_m(\theta)\left[1 - 3\left(\frac{r-r_i}{r_j-r_i}\right)^2 + 2\left(\frac{r-r_i}{r_j-r_i}\right)^3\right],$$

$$N_{2,\theta\theta} = \Theta''_m(\theta)(r-r_i)\left[1 - 2\frac{r-r_i}{r_j-r_i} + \left(\frac{r-r_i}{r_j-r_i}\right)^2\right],$$

$$N_{3,\theta\theta} = \Theta''_m(\theta)\left(\frac{r-r_i}{r_j-r_i}\right)^2\left(3 - 2\frac{r-r_i}{r_j-r_i}\right), \quad N_{4,\theta\theta} = \Theta''_m(\theta)\frac{(r-r_i)^2}{r_j-r_i}\left(\frac{r-r_i}{r_j-r_i} - 1\right),$$

$$N_{p+4,\theta\theta} = \Theta''_m(\theta)\frac{r-r_i}{r_j-r_i}\left(1 - \frac{r-r_i}{r_j-r_i}\right)\sin\left(\frac{r-r_i}{r_j-r_i}p\pi\right).$$

References

[1] A.W. Leissa, Vibration of Plates, NASA SP-160, Office of Technology Utilization, NASA, Washington, 1969.

[2] C. Rubin, Nodal circles and natural frequencies for the isotropic wedge, *Journal of Sound and Vibration* 39 (1975) 523–526.

[3] R.A. Westmann, A note on free vibrations of triangular and sector plates, *Journal of the Aerospace Sciences* 29 (1962) 1139–1140.

[4] C.S. Kim, S.M. Dickinson, On the free, transverse vibration of annular and circular, thin, sectorial plates subject to certain complicating effects, *Journal of Sound and Vibration* 134 (1989) 407–421.

[5] G.K. Ramaiah, K. Vijayakumar, Natural frequencies of circumferentially truncated sector plates with simply supported straight edges, *Journal of Sound and Vibration* 34 (1974) 53–61.

[6] H.B. Khurasia, S. Rawtani, Vibration analysis of circular segment shaped plates, *Journal of Sound and Vibration* 67 (1979) 307–313.

[7] Y.K. Cheung, M.S. Cheung, Flexural vibrations of rectangular and other polygonal plates, *Journal of the Engineering Mechanics Division* 97 (1971) 391–411.

[8] O.C. Zienkiewicz, R.L. Taylor, *The Finite Element Method*, Vol. 1, fourth ed., McGraw-Hill, New York, 1989.

[9] A.Y.T. Leung, J.K.W. Chan, Fourier *p*-element for the analysis of beams and plates, *Journal of Sound and Vibration* 212 (1998) 179–185.

[10] A. Houmat, A sector Fourier *p*-element applied to free vibration analysis of sectorial plates, *Journal of Sound and Vibration* 243 (2001) 269–282.

[11] Y.K. Cheung, *Finite Strip Method in Structural Analysis*, Pergamon, Oxford, 1976.

[12] M.S. Cheung, M.Y.T. Chan, Static and dynamic of thin and thick sectorial plates by finite strip method, *Computers and Structures*, 1981.

[13] T. Mizusawa, T. Kajita, Vibration of annular sector plates using spline strip method, *Communications in Applied Numerical Methods*, 1992.

[14] A.Y.T. Leung, *Dynamic Stiffness and Substructures*, Springer, London, 1993.

[15] O.G. Mcgee, A.W. Leissa, C.S. Huang, Vibration of completely free sectorial plates, *Journal of Sound and Vibration* 164 (1993) 565–569.

[16] A.W. Leissa, Y. Narita, Natural frequencies of simply supported circular plates, *Journal of Sound and Vibration* 70 (1980) 221–229.